SIAM J. APPL. MATH.
Vol. 83, No. 1, pp. 254-275

AN EULERIAN NONLINEAR ELASTIC MODEL FOR COMPRESSIBLE AND FLUIDIC TISSUE WITH RADIALLY SYMMETRIC GROWTH*

CHAOZHEN WEI†‡ AND MIN WU‡

Abstract. Cell proliferation, apoptosis, and myosin-dependent contraction can generate elastic stress and strain in living tissues, which may be dissipated by internal rearrangement through cell topological transition and cytoskeletal reorganization. Moreover, cells and tissues can change their sizes in response to mechanical cues. The present work demonstrates the role of tissue compressibility and internal rearranging activities on its size and mechanics regulation in the context of differential growth induced by a field of growth-promoting chemical factors. We develop a mathematical model based on finite elasticity and growth theory and the reference map techniques to describe the coupled tissue growth and mechanics in the Eulerian frame. We incorporate the tissue rearrangement by introducing a rearranging rate to the reference map evolution, leading to elastic-energy dissipation when tissue growth and deformation are in radial symmetry. By linearizing the model, we show that the stress follows the Maxwell-type viscoelastic relaxation. The rearrangement rate, which we call tissue fluidity, sets the stress relaxation time, and the ratio between the shear modulus and the fluidity sets the tissue viscosity. By nonlinear simulation of growing tissue spheroids and discs with graded growth rates along the radius, we find that the tissue compressibility and fluidity influence their equilibrium size. By comparing the nonlinear simulations with the linear analytical solutions, we show the size change as a nonlinear effect due to the advection of the tissue density flow, which only occurs when both tissue compressibility and fluidity are small. We apply the model to study tumor spheroid growth and epithelial disc growth when a reaction-diffusion process determines the growth-promoting factor field.

Key words. soft tissue, differential growth, nonlinear elasticity, Eulerian framework, tissue fluidity, tissue compressibility

MSC codes. 35Q74, 92-10, 92C10, 74Bxx, 74L15

DOI. 10.1137/21M1463653

1. Introduction.

The interaction between cell activities and tissue mechanics plays an essential role during development, homeostasis, and cancer progression. Mechanical stresses can arise and accumulate in growing tissues due to inhomogeneous cell proliferation and apoptosis and can be dissipated by rearranging activities such as cell neighbor exchange, oriented cell division, and cell extrusion [30, 23, 32]. Not only do cell activities generate mechanical forces, but tissue growth also responds to local stress and strain, such as in growing tumor spheroids [25, 38, 12] and *Drosophila* wing discs [1, 33]. In light of increasing evidence and attention to the interaction between growth and mechanics, the present study seeks to improve our analytical understanding of the role of tissue mechanical properties in size and mechanics regulation.

Over the last three decades, the theory of finite elasticity and growth [42], also called morphoelasticity [21], has become a powerful tool to understand tissue growth

* Received by the editors December 7, 2021; accepted for publication (in revised form) October 5, 2022; published electronically February 27, 2023.
https://doi.org/10.1137/21M1463653
Funding: The work of the second author was supported by NSF-DMS-2012330 and 2144372.

† School of Mathematical Sciences, University of Electronic Science and Technology of China, Chengdu, Sichuan 611731, China (cwei4@uestc.edu.cn).

‡ Department of Mathematical Sciences, Worcester Polytechnic Institute, Worcester, MA 01609 USA (englier@gmail.com).

and mechanics, especially for soft tissues [16]. The heart of the theory is to decompose the deformation gradient into a growth stretch tensor followed by an elastic deformation tensor. The growth tensor captures the local volumetric growth due to new material production, while the elastic deformation tensor captures the mechanical response of the tissue continuum to maintain its integrity and results in residual stress. Within this framework, specific models have been developed to understand growth and morphogenesis in various scenarios, such as the formation of gut lumen ridges [34, 45, 2] and brain convolutions [7, 48], tumor growth [22] and pathological cardiac growth [20], the re-epithelialization of the adult skin wound [50], etc. The interested reader is referred to the recent reviews [27, 3] and the book [21] for more examples.

Since cells undergo growth, division, and apoptosis in response to their inherited drives and environmental cues, tissue growth depends on both the material (inherited) and the spatial (environmental) coordinates. Most previous finite elasticity and growth models considered the dependence of growth on the material coordinates, except in [22] to the best of our knowledge. The Lagrangian description makes it difficult to study the interaction between tissue growth and environmental cues, such as the direct coupling between the tissue growth rate and the reaction-diffusion process of the growth-promoting factors (e.g., [11]). For previous tumor-growth models that considered the coupling of finite elasticity and growth with nutrient transport [4, 51], the nutrient transport modeled in Lagrangian coordinates resulted in convoluted formulation due to the transformation of the gradient and divergence operators from the material coordinates to spatial coordinates.

Recently, one of us has developed an Eulerian model of incompressible tissue growth and elasticity [52] by using reference map techniques [10, 28]. Reference map techniques reconstruct the deformation gradient based on the reference map, the inverse of the motion, instead of describing the dynamics of the deformation gradient in the Eulerian frame [36, 35]. We have applied this formulation to understand the regulation of tumor spheroid size and mechanics through diffusive growth-promoting factors and growth-inhibiting mechanical feedbacks, in which the steady-state size of the tumor decreases when the strength of external physical confinement [25] and compression [38, 12] are elevated. In addition, the Eulerian model enabled us to account for the tissue rearranging activities by modifying the evolution equation of the reference map, which results in a Maxwell-type stress relaxation. This Eulerian approach based on a reference map is simpler from the computational perspective than the previous Maxwell-type models for stress relaxation (e.g., [41, 46]). In [52], we have considered the tumor as incompressible, and the volume loss in response to mechanical compression [12] is an active process due to cell water efflux [24]. Alternatively, the cell and tissue can be considered as compressible material with measurable bulk moduli [24, 40], which can change volume and density passively to local stress.

In this paper, we develop an Eulerian model of tissue growth and elasticity considering its compressibility and rearranging activities. We assume that the soft tissues are compressible neo-Hookean materials with an isotropic growth rate in response to spatial stimuli and a rearrangement rate which changes their reference positions. With radially symmetric growth, we show that the rearranging activities in our formulation dissipate the stored elastic energy and enable the model to behave like a linear Maxwell viscoelastic model when the rearrangement rate is larger than the growth rate. By presenting linear analysis and nonlinear simulations for our model, we demonstrate the synergic effect of tissue compressibility and internal rearrangement on tissue size and mechanics regulation, and apply the model to study tumor

spheroid growth and epithelial disc growth when the growth-promoting factor field is determined by a reaction-diffusion process.

This paper is organized as follows. In section 2, we present our Eulerian model with compressible tissue growth and elasticity using reference map techniques. In section 3, we introduce the rearranging activity in the reference map evolution equation in radial symmetry and derive the evolution equations of the elastic deformation and the strain energy. In section 4, we linearize the model when the time scale of rearranging activity is much shorter than that of the growth in radial symmetry. We show that the linearized model behaves like the Maxwell viscoelastic model at the time scale of rearrangement rate and like viscous fluid at the time scale of growth. In section 5, we show the synergic effect of tissue compressibility and rearrangement on tissue size and mechanics by presenting the steady-state analytical solution for the linearized model and performing numerical simulations for the nonlinear model. In section 6, we apply our nonlinear model to investigate tumor growth where the growth rate is coupled with a growth-promoting factor field determined by a reaction-diffusion process. In section 7, we summarize and discuss our results.

2. Growing tissues as compressible elastic material.

2.1. Decomposition of deformation gradient. We consider a region of soft tissues initially in a stress-free reference configuration $\mathcal{B}_0 \subset \mathbb{R}^d$ ($d = 2$ or 3). The mapping $\boldsymbol{\chi} : \mathcal{B}_0 \to \mathcal{B}_t$ is introduced to relate the stress-free initial reference configuration $\mathcal{B}_0$ to the current deformed configuration $\mathcal{B}_t$ via $\mathbf{x} = \boldsymbol{\chi}(\mathbf{X}, t)$, where $\mathbf{x} \in \mathcal{B}_t$ is the current location at time t of a particle initially located at $\mathbf{X} \in \mathcal{B}_0$. The tangent map of $\boldsymbol{\chi}$ is denoted by $\mathbf{F} = \partial \mathbf{x}/\partial \mathbf{X}$, the *geometric deformation gradient*.

In the theory of finite elasticity and growth [42], we can decompose the geometric deformation gradient by

$$\mathbf{F} = \mathbf{F}_e \mathbf{F}_g, \tag{2.1}$$

where $\mathbf{F}_g$ is the accumulated *growth stretch tensor* describing the stretch relative to the reference configuration due to stress-free volumetric tissue growth, which may result in an intermediate incompatible configuration $\mathcal{B}_g \subset R^d$. $\mathbf{F}_g$ can be interpreted as the tangent of the mapping from $\mathcal{B}_0$ to $\mathcal{B}_g \subset R^D$ ($D > d$) when $\mathcal{B}_g$ is a differential manifold. Instead of adding new material points, the growth stretch tensor $\mathbf{F}_g$ captures the change of size and shape of the local macroscopic continuum due to the growth. The *elastic deformation tensor* $\mathbf{F}_e$ describes the elastic response of the tissue material and maps the tangent space of $\mathcal{B}_g$ to that of $\mathcal{B}_t$. Figure 1(a) illustrates this decomposition of geometric deformation gradient. The idea was developed much earlier in research communities other than biomechanics [43] and is frequently called the Kröner–Lee decomposition in elastoplasticity [29, 31].

2.2. Dynamics of reference map and deformation gradient. Instead of describing the geometric deformation map $\boldsymbol{\chi}(\mathbf{X}, t)$ in the Lagrangian frame, we introduce a system of finite elasticity and growth in the Eulerian frame by using the *reference map* [10, 28], $\mathbf{X} = \mathbf{Y}(\mathbf{x}, t) := \boldsymbol{\chi}^{-1}(\mathbf{x}, t)$, which is the inverse of the motion $\boldsymbol{\chi}$. Since the initial reference coordinates of a material point do not change in time, we have $d\mathbf{X}/dt = 0$, where $df/dt = \partial f(\mathbf{X}, t)/\partial t$ is the material time derivative of any function f. Letting $\mathbf{v}(\mathbf{x}, t) = \frac{\partial}{\partial t}\boldsymbol{\chi}(\mathbf{X}, t)$ be the material velocity, and using the chain rule, we obtain the dynamics of reference map (with the initial condition)

$$\frac{d\mathbf{X}}{dt} = \frac{\partial \mathbf{Y}}{\partial t}(\mathbf{x}, t) + \mathbf{v} \cdot \nabla \mathbf{Y}(\mathbf{x}, t) = \mathbf{0} \text{ with } \mathbf{Y}(\mathbf{x}, 0) = \mathbf{x}. \tag{2.2}$$

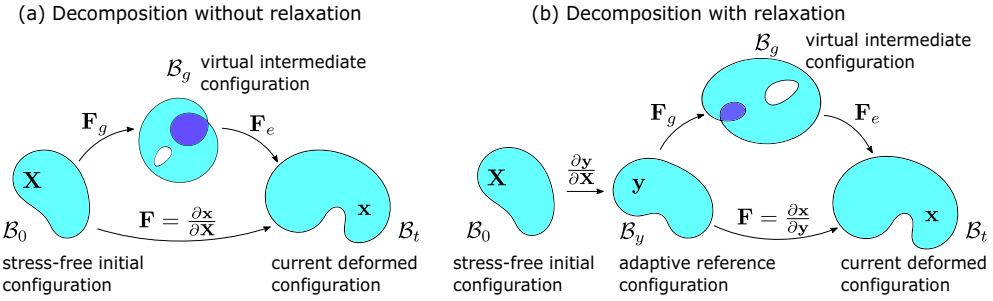

FIG. 1. *Decomposition of the geometric deformation gradient into growth stretch tensor and elastic deformation tensor.* (a) *Loop* $\mathcal{B}_0 \to \mathcal{B}_g \to \mathcal{B}_t$*: decomposition of the geometric deformation with respect to stress-free initial configuration.* (b) *loop* $\mathcal{B}_0 \to \mathcal{B}_y \to \mathcal{B}_g \to \mathcal{B}_t$*: relaxation of initial configuration to adaptive reference configuration and the decomposition of the geometric deformation with respect to adaptive reference configuration.*

We can show that (2.2) leads to the dynamics of the geometric deformation gradient $\mathbf{F} = \partial \mathbf{x}/\partial \mathbf{X} = (\partial \mathbf{X}/\partial \mathbf{x})^{-1} = (\nabla \mathbf{Y})^{-1}$ (where $\nabla = \nabla_{\mathbf{x}}$) [10, 28]. By taking ∇ on both sides of (2.2), we obtain the evolution of $d(\nabla \mathbf{Y})/dt = \partial(\nabla \mathbf{Y})/\partial t + \mathbf{v} \cdot \nabla(\nabla \mathbf{Y}) = -\nabla \mathbf{Y} \nabla \mathbf{v}$. Together with the relation $d(\nabla \mathbf{Y}^{-1})/dt = -\nabla \mathbf{Y}^{-1}(d(\nabla \mathbf{Y})/dt)\nabla \mathbf{Y}^{-1}$, we obtain the evolution of $(\nabla \mathbf{Y})^{-1}$

$$\frac{d(\nabla \mathbf{Y})^{-1}}{dt} = \frac{\partial(\nabla \mathbf{Y})^{-1}}{\partial t} + \mathbf{v} \cdot \nabla(\nabla \mathbf{Y})^{-1} = \nabla \mathbf{v}(\nabla \mathbf{Y})^{-1} \text{ with } (\nabla \mathbf{Y})^{-1}(\mathbf{x}, 0) = \mathbf{I}, \tag{2.3}$$

which is equivalent to the Lagrangian formalism $d\mathbf{F}/dt = \nabla \mathbf{v}\mathbf{F}$ with $\mathbf{F}(\mathbf{X}, 0) = \mathbf{I}$. Following this, we can obtain the evolution of the local volumetric (when $d = 3$) or areal (when $d = 2$) variation $J = \det(\mathbf{F}) = \det(\nabla \mathbf{Y})^{-1}$. Using the chain rule $dJ/dt = [\partial J/\partial(\nabla \mathbf{Y})^{-1}] : [d(\nabla \mathbf{Y})^{-1}/dt]$ (where $A : B = A_{ij}B_{ij}$ is the Frobenius inner product of two matrices represented in Einstein notation) and the relation $\partial J/\partial(\nabla \mathbf{Y})^{-1} = J(\nabla \mathbf{Y})^{\mathrm{T}}$, we obtain

$$\frac{dJ}{dt} = \frac{\partial J}{\partial t} + \mathbf{v} \cdot \nabla J = J \nabla \cdot \mathbf{v} \text{ with } J(\mathbf{x}, 0) = 1, \tag{2.4}$$

where $\nabla \cdot \mathbf{v}$ represents the rate of local volumetric (when $d = 3$) or areal (when $d = 2$) expansion. The above derivations, which lead to (2.3) and (2.4), demonstrate that the dynamics of $\mathbf{Y}$ in (2.2) implies the dynamics of $\mathbf{F} = (\nabla \mathbf{Y})^{-1}$ and $J = \det \mathbf{F}$. Thus, we only need to trace the evolution of $\mathbf{Y}$ (2.2), rather than explicitly solve (2.3) and (2.4) in this Eulerian formulation.

2.3. Dynamics of active growth. According to the decomposition equation (2.1), the local volume variation $J = J_g J_e$, where $J_g = \det(\mathbf{F}_g)$, *the active volume variation* due to growth, and $J_e = \det(\mathbf{F}_e)$, *the elastic volume variation* due to elastic deformation. Defining the current tissue density $\rho(\mathbf{x}, t)$ (mass per current unit volume), by change of variable, we have

$$\int_{\Omega_t} \rho dV_t = \int_{\Omega_0} \rho J dV_0, \tag{2.5}$$

where $\Omega_t \subset \mathcal{B}_t$ denotes an arbitrary current region and coincides with $\Omega_0 \subset \mathcal{B}_0$ at $t = 0$, and $dV_t \subseteq \mathcal{B}_t$ ($dV_0 \subseteq \mathcal{B}_0$) denotes the infinitesimal volume element in the current (initial stress-free) configuration.

To describe the evolution of growth, we consider

$$\frac{d}{dt}\int_{\Omega_t} \rho \, dV_t = \int_{\Omega_t} \rho\gamma \, dV_t, \tag{2.6}$$

where $\gamma(\mathbf{x}, t)$ is the rate of mass production or loss due to cell proliferation and apoptosis, which can depend on the spatial coordinates $\mathbf{x}$ via chemical and mechanical factor regulations [25, 38, 12, 1, 33]. By the Reynolds transport theorem and the arbitrariness of Ω_t, we obtain the equation of mass balance with source

$$\frac{d\rho}{dt} = \frac{\partial \rho}{\partial t} + \mathbf{v}\cdot\nabla\rho = \rho(\gamma - \nabla\cdot\mathbf{v}) \text{ with } \rho(\mathbf{x}, 0) = \rho_0, \tag{2.7}$$

where ρ_0 is the initial stress-free tissue density.

To consider mass balance between the initial stress-free configuration and the current configuration, we assume that the stress-free density ρ_0 remains constant during growth [27]. That is, the change of mass is only attributed to the active volume variation J_g; the elastic volume variation J_e only changes the local density and volume element but not the mass. After active growth, the volume element dV_0 is modified into $J_g dV_0$, and ρ and ρ_0 are connected by

$$\int_{\Omega_t} \rho dV_t = \int_{\Omega_0} \rho_0 (J_g dV_0). \tag{2.8}$$

Combining (2.5) and (2.8), we obtain the relation between densities

$$\rho J = \rho_0 J_g \tag{2.9}$$

due to the arbitrariness of Ω_0. Together with the relation $J = J_g J_e$, we have $J_e = \rho_0/\rho$.

By the assumption of constant ρ_0 and combining (2.4), (2.7), and (2.9), we obtain the evolution of the active volume variation

$$\frac{dJ_g}{dt} = \frac{\partial J_g}{\partial t} + \mathbf{v}\cdot\nabla J_g = \gamma J_g \text{ with } J_g(\mathbf{x}, 0) = 1. \tag{2.10}$$

One can see that under the assumption that ρ_0 remains constant during growth, the rates of mass production and active volumetric growth (when $d = 3$) or areal growth (when $d = 2$) are identical, both being γ. Notice within this macroscopic continuum framework, the new material production is described by the rate of change of J_g at a material point, which does not involve the addition or removal of material points in time. For simplicity, we assume the growth stretch tensor $\mathbf{F}_g = J_g^{1/d}\mathbf{I}$ to be isotropic such that its dynamics is determined by (2.10). We define the isotropic growth rate tensor

$$\mathbf{\Gamma}_{iso} := \frac{d\mathbf{F}_g}{dt}\mathbf{F}_g^{-1} = \frac{\gamma}{d}\mathbf{I}. \tag{2.11}$$

2.4. Dynamics of elastic deformation. By the relation $\mathbf{F}_e = \mathbf{F}\mathbf{F}_g^{-1} = J_g^{-1/d}\nabla\mathbf{Y}^{-1}$ and (2.3) and (2.10), we obtain the evolution of $\mathbf{F}_e$

$$\frac{d\mathbf{F}_e}{dt} = \frac{\partial \mathbf{F}_e}{\partial t} + \mathbf{v}\cdot\nabla\mathbf{F}_e = (\nabla\mathbf{v} - \mathbf{\Gamma}_{iso})\mathbf{F}_e \text{ with } \mathbf{F}_e(\mathbf{x}, 0) = \mathbf{I}, \tag{2.12}$$

which yields the dynamics of the elastic volume (when $d = 3$) or areal (when $d = 2$) variation

$$\frac{dJ_e}{dt} = \frac{\partial J_e}{\partial t} + \mathbf{v}\cdot\nabla J_e = J_e(\nabla\cdot\mathbf{v} - \gamma) \text{ with } J_e(\mathbf{x}, 0) = 1. \tag{2.13}$$

The evolution of J_e is consistent with the relation $J_e = \rho_0/\rho$ and (2.7). The above derivations demonstrate that the dynamics of $\mathbf{Y}$ and J_g in (2.2) and (2.10) imply the dynamics of $\mathbf{F}_e = J_g^{-1/d}(\nabla \mathbf{Y})^{-1}$, $J_e = \det \mathbf{F}_e$, and $\rho = \rho_0/J_e$. Thus, mass balance and elastic deformation dynamics are ensured by solving (2.2) and (2.10) in this Eulerian formulation.

2.5. Compressible neo-Hookean elasticity. For simplicity, we treat soft tissues as isotropic, compressible neo-Hookean elastic material. The strain energy density function (per unit stress-free volume) in d-dimensions is given by [47]

$$W(\mathbf{F}_e) = \frac{1}{2}\mu(\bar{I}_1 - d) + \frac{1}{2}K(J_e - 1)^2, \tag{2.14}$$

where μ and K are, respectively, the shear and bulk modulus, and $\bar{I}_1 = J_e^{-2/d}\mathrm{Tr}(\mathbf{C}_e)$ is the first invariant of the isochoric part $\bar{\mathbf{C}}_e = J_e^{-1/d}\mathbf{C}_e$ of the *right Cauchy–Green elastic deformation tensor* $\mathbf{C}_e = \mathbf{F}_e^{\mathrm{T}}\mathbf{F}_e$.

To derive the stress-strain constitutive relation for compressible elastic body with growth, we consider the total strain energy of a region $\Omega_t \subseteq \mathcal{B}_t$

$$E(t) = \int_{\Omega_t} J_e^{-1} W(\mathbf{F}_e) dV_t, \tag{2.15}$$

where the factor J_e^{-1} accounts for the ratio of the stress-free volume element after growth $J_g dV_0$ to the deformed volume element $dV = J dV_0$. Taking the material time derivative of $E(t)$ leads to

$$\begin{aligned}
\frac{dE}{dt} &= \int_{\Omega_t} \Big(\frac{d}{dt}(J_e^{-1}W) + J_e^{-1} W \nabla \cdot \mathbf{v} \Big) dV_t \\
&= \int_{\Omega_t} \Big(J_e^{-1} \frac{\partial W}{\partial \mathbf{F}_e} : \frac{d\mathbf{F}_e}{dt} - J_e^{-2} W \frac{dJ_e}{dt} + J_e^{-1} W \nabla \cdot \mathbf{v} \Big) dV_t \\
&= \int_{\Omega_t} \Big(J_e^{-1} \frac{\partial W}{\partial \mathbf{F}_e} \mathbf{F}_e^{\mathrm{T}} : \nabla \mathbf{v} - J_e^{-1} \frac{\partial W}{\partial \mathbf{F}_e} \mathbf{F}_e^{\mathrm{T}} : \mathbf{\Gamma}_{iso} + J_e^{-1} W \gamma \Big) dV_t,
\end{aligned} \tag{2.16}$$

where we have used the evolution equations (2.12) and (2.13) in the last line. We assume that the growth does not interfere with the elasticity of tissue material. When $\gamma = 0$ and $\mathbf{\Gamma}_{iso} = \mathbf{0}$, we obtain the constitutive relation for the *Cauchy stress tensor*

$$\begin{aligned}
\boldsymbol{\sigma} &= J_e^{-1} \frac{\partial W}{\partial \mathbf{F}_e} \mathbf{F}_e^{\mathrm{T}} \\
&= \mu J_e^{-\frac{2+d}{d}} \Big(\mathbf{F}_e \mathbf{F}_e^{\mathrm{T}} - \frac{I_1}{d} \mathbf{I} \Big) + K(J_e - 1)\mathbf{I} \\
&= \mu J_g J^{-\frac{2+d}{d}} \Big(\nabla \mathbf{Y}^{-1} \nabla \mathbf{Y}^{-\mathrm{T}} - \frac{\tilde{I}_1}{d} \mathbf{I} \Big) + K(J_g^{-1} J - 1)\mathbf{I},
\end{aligned} \tag{2.17}$$

where $I_1 = \mathrm{Tr}(\mathbf{C}_e)$ and $\tilde{I}_1 = \mathrm{Tr}(\mathbf{C})$ where $\mathbf{C} = \nabla \mathbf{Y}^{-\mathrm{T}} \nabla \mathbf{Y}^{-1} = \mathbf{F}^T \mathbf{F}$ is the *right Cauchy–Green deformation tensor*. The stress can be decomposed as $\boldsymbol{\sigma} = \boldsymbol{\sigma}_s + \boldsymbol{\sigma}_p$, the sum of the deviatoric part $\boldsymbol{\sigma}_s$ (proportional to μ) and the isotropic part $\boldsymbol{\sigma}_p$ (proportional to K). For incompressible materials, i.e., $J_e \equiv 1$, the isotropic part of the stress vanishes. Instead, a pressure term should be introduced (as a Lagrangian multiplier) for maintaining incompressibility [52].

2.6. Dynamics of growing tissue without relaxation. Recognizing the constitutive stress-strain relation, the rate of change of total strain energy reduces to

$$\frac{dE}{dt} = \int_{\Omega_t} J_e^{-1} W \gamma dV_t - \int_{\Omega_t} \boldsymbol{\sigma}_p : \boldsymbol{\Gamma}_{iso} dV_t - \int_{\Omega_t} (\nabla \cdot \boldsymbol{\sigma}) \cdot \mathbf{v} dV_t + \int_{\partial\Omega_t} \mathbf{v} \cdot (\boldsymbol{\sigma} \cdot \mathbf{n}) dS_t, \tag{2.18}$$

where $\mathbf{n}$ is the outward unit normal of the boundary $\partial\Omega_t$ and we have used the relations $\boldsymbol{\sigma} : \boldsymbol{\Gamma}_{iso} = \boldsymbol{\sigma}_p : \boldsymbol{\Gamma}_{iso}$, $\boldsymbol{\sigma} : \nabla \mathbf{v} = \nabla \cdot (\boldsymbol{\sigma} \cdot \mathbf{v}) - (\nabla \cdot \boldsymbol{\sigma}) \cdot \mathbf{v}$, and the divergence theorem. The first term on the right-hand side represents the change of elastic energy due to the addition of material by volumetric (or areal) growth. Without the minus sign, the second term represents the stress power due to active isotropic growth, similar to the stress power due to local geometric volumetric (or areal) expansion, except that $\boldsymbol{\sigma}_p$ is conjugated with isotropic growth rate tensor $\boldsymbol{\Gamma}_{iso}$ instead of local volumetric (or areal) expansion $(\nabla \cdot \mathbf{v})\mathbf{I}$. This shows that the active growth ($\gamma > 0$) in the compressed tissue ($\mathrm{Tr}(\boldsymbol{\sigma}_p) < 0$) requires the addition of energy. The third and fourth terms represent the stress power (due to the motion) in the bulk and at the boundary. In the theory of finite elasticity and growth [42], the body force and inertial force are often assumed to be negligible. Following this assumption, we obtain the equation of mechanical equilibrium

$$\nabla \cdot \boldsymbol{\sigma} = \mathbf{0} \tag{2.19}$$

in the tissue bulk Ω_t. At the fixed boundary Σ_D, we prescribe

$$\mathbf{v} = \mathbf{0}, \tag{2.20}$$

and at the free boundary Σ_t, we prescribe

$$\boldsymbol{\sigma} \cdot \mathbf{n} = \mathbf{0}. \tag{2.21}$$

Combining the evolution equations (2.2) and (2.10) with their initial conditions, the constitutive relation (2.17), the mechanical equilibrium equation (2.19), and the boundary condition equations (2.20) and (2.21), we establish a coupled nonlinear system for describing the tissue growth and mechanics without stress relaxation.

3. Tissue rearrangement and stress relaxation. At the large-scale continuum level, soft tissues are effectively viscoelastic due to cell neighbor exchanges [30, 32] and cytoskeleton reorganization [14] at the cell and subcellular levels. Therefore, the stress caused by differential growth can be effectively relaxed; otherwise, the stress may accumulate and blow up. In the theory of finite elasticity and growth, stress-dependent growth rate can be used to drive the stress relaxation to a specified target stress [47]. One could also extend the traditional theory by introducing viscoelastic mechanisms to relax elastic strains (the Kelvin–Voigt model) or stresses (the Maxwell model) [37, 13]. In addition, anisotropic growth due to orientated cell divisions and apoptosis may effectively alleviate the accumulated stress and introduce "fluidity" in the tissue mechanics [6, 41]. Following [52], we will consider the stress relaxation mechanism for compressible tissues by modifying the reference map evolution. The new development in this section is to derive the evolution equation for the "adaptive" active volume variation J_g, which is implicitly satisfied in the incompressible case (see below) and prove that our relaxation mechanism dissipates the stored strain energy where rotation can be neglected.

3.1. Adaptive reference map. We describe the tissue rearranging activities by introducing an "adaptive" reference configuration $\mathcal{B}_y$ that relaxes from the initial reference configuration $\mathcal{B}_0$ and adapts to the current deformed configuration $\mathcal{B}_t$. We describe the "relaxed" reference coordinates by the adaptive reference map $\mathbf{Y}:\mathcal{B}_t \to \mathcal{B}_y$ via $\mathbf{y} = \mathbf{Y}(\mathbf{x}, t)$ for a particle currently located at $\mathbf{x} \in \mathcal{B}_t$ and initially located at $\mathbf{X} \in \mathcal{B}_0$. Henceforth we will use the same notation as in section 2 to represent all tensors and their determinant in the presence of tissue rearrangement (i.e., with respect to the adaptive reference configuration). The relation of the adaptive reference $\mathcal{B}_y$ with $\mathcal{B}_0$ and $\mathcal{B}_t$ is illustrated in Figure 1(b).

Now we can define the effective deformation gradient $\mathbf{F} = \partial\mathbf{x}/\partial\mathbf{y} = \nabla\mathbf{Y}^{-1}$ with respect to the adaptive reference configuration $\mathcal{B}_y$. In general, $\mathbf{F} = \mathbf{RU}$ by the polar decomposition, where $\mathbf{U} = \sqrt{\mathbf{F}^T\mathbf{F}} = \sqrt{\mathbf{C}}$ is the symmetric positive-definite stretch tensor and $\mathbf{R} = \mathbf{FU}^{-1}$ is the orthogonal rotation tensor. For the symmetric tissue growth, such as tumor spheroid growth or circular wound closure processes, $\mathbf{R} = \mathbf{I}$. Henceforth, for simplicity, we will focus our discussion on the tissue growth with rearrangement where rotation can be neglected, and therefore we will write the deformation gradient $\mathbf{F} = \nabla\mathbf{Y}^{-1} = \mathbf{U}$ and the elastic deformation tensor $\mathbf{F}_e = \sqrt{\mathbf{C}_e} = \mathbf{U}_e$, the elastic stretch tensor. The system with rotation ($\mathbf{R} \neq \mathbf{I}$) is discussed in the supplementary materials (Supplementary_Materials_r3.pdf [local/web 655KB]).

3.2. Dynamics with tissue rearrangement. The dynamics of the adaptive reference map $\mathbf{y} = \mathbf{Y}(\mathbf{x}, t)$ in Eulerian frame is given by

$$\frac{d\mathbf{y}}{dt} = \frac{\partial\mathbf{Y}}{\partial t} + \mathbf{v}\cdot\nabla\mathbf{Y} = \beta(\mathbf{x}-\mathbf{y}) \text{ with } \mathbf{Y}(\mathbf{x},0) = \mathbf{x}, \tag{3.1}$$

where β is the rate of rearrangement that measures how fast the reference configuration of the tissue adapts to the current configuration. The physical reasoning is that if the reference configuration adapts to the current configuration instantaneously ($\beta \to \infty$), there should not be elastic strain and stress stored in the growing tissue. Here we consider it as spatially uniform for simplicity. See the summary and discussion, section 7, for future considerations of nonuniform β. When $\beta \neq 0$, this evolution equation can be rewritten as the relaxation of $\mathbf{u} = \mathbf{x} - \mathbf{y}$ with decaying rate β, $d\mathbf{u}/dt = \mathbf{v} - \beta\mathbf{u}$. We call $\mathbf{u}$ the *adaptive displacement* henceforth, since $\mathbf{u}$ does not follow the original relation between displacement and velocity $d\mathbf{u}/dt = \mathbf{v}$ when $\beta \neq 0$. When $\beta = 0$, we recover the dynamics of the original reference map without tissue arrangement in (2.2) and the relation $d\mathbf{u}/dt = \mathbf{v}$.

Following a similar derivation process in section 2, the dynamics of adaptive reference map (3.1) leads to the dynamics of the relaxed deformation gradient $\nabla\mathbf{Y}^{-1} = \mathbf{U}$

$$\frac{\partial\mathbf{U}}{\partial t} + \mathbf{v}\cdot\nabla\mathbf{U} = [\nabla\mathbf{v} - \beta(\mathbf{U}-\mathbf{I})]\mathbf{U} \text{ with } \mathbf{U}(\mathbf{x},0) = \mathbf{I}. \tag{3.2}$$

The term with β demonstrates the relaxation of the deformation gradient in response to the *Biot strain tensor* $(\mathbf{U}-\mathbf{I})$. This equation further leads to the evolution of the relaxed volume variation $J = \det\mathbf{U}$

$$\frac{dJ}{dt} = \frac{\partial J}{\partial t} + \mathbf{v}\cdot\nabla J = J\big[\nabla\cdot\mathbf{v} - \beta\mathrm{Tr}(\mathbf{U}-\mathbf{I})\big] \text{ with } J(\mathbf{x},0) = 1. \tag{3.3}$$

We assume that the tissue rearranging activities do not interfere the dynamics of tissue density ρ or the initial stress-free density ρ_0 (mass is conserved with considering

rearrangement). Combining (2.7) and (2.9) with the adaptive evolution of J, (3.3), the evolution of adaptive J_g should follow

$$\frac{dJ_g}{dt} = \frac{\partial J_g}{\partial t} + \mathbf{v}\cdot\nabla J_g = J_g\big[\gamma - \beta \mathrm{Tr}(\mathbf{U}-\mathbf{I})\big] \text{ with } J_g(\mathbf{x},0) = 1. \tag{3.4}$$

When strict incompressibility is imposed ($J_e = J/J_g = 1$ in [52]), comparing (3.4) with (3.3) yields the constraint $\nabla\cdot\mathbf{v} = \gamma$. In fact, (3.4) is equivalent to $\nabla\cdot\mathbf{v} = \gamma$ when $J_e = J/J_g = 1$ is given. Thus, (3.4) describes the dynamics of J_g in both compressible and incompressible rearranging tissues.

Assuming that the adaptive growth stretch tensor $\mathbf{F}_g = J_g^{1/d}\mathbf{I}$ is still isotropic, the dynamics of the adaptive elastic stretch tensor $\mathbf{U}_e = \mathbf{F}_e = J_g^{-1/d}\mathbf{U}$ follows

$$\frac{d\mathbf{U}_e}{dt} = \frac{\partial \mathbf{U}_e}{\partial t} + \mathbf{v}\cdot\nabla\mathbf{U}_e = \left[(\nabla\mathbf{v} - \mathbf{\Gamma}_{iso}) - \beta\left(\mathbf{U} - \frac{1}{d}\mathrm{Tr}(\mathbf{U})\mathbf{I}\right)\right]\mathbf{U}_e \text{ with } \mathbf{U}_e(\mathbf{x},0) = \mathbf{I}. \tag{3.5}$$

The term with β is the simplification of $[(\mathbf{U}-\mathbf{I}) - \frac{1}{d}\mathrm{Tr}(\mathbf{U}-\mathbf{I})\mathbf{I}]$, showing the relaxation of $\mathbf{U}_e$ due to the deviatoric components of the Biot tensor. One can check that the volumetric change due to elastic deformation $J_e = \det(\mathbf{U}_e)$ yields the same dynamics $dJ_e/dt = J_e(\nabla\cdot\mathbf{v} - \gamma)$ as in (2.13) and the relation $\rho J_e = \rho_0$ still holds.

Substituting (2.13) and (3.5) into (2.16), we obtain the rate of change of the total strain energy

$$\frac{dE}{dt} = \int_{\Omega_t}\Big(J_e^{-1}W\gamma + \boldsymbol{\sigma} : (\nabla\mathbf{v} - \mathbf{\Gamma}_{iso})\Big)dV_t - \beta\int_{\Omega_t}\boldsymbol{\sigma}_s : \left(\mathbf{U} - \frac{1}{d}\mathrm{Tr}(\mathbf{U})\mathbf{I}\right)dV_t.$$

The first integral represents the same energy change due to active growth as in (2.18). The second integral with β represents the energy change due to tissue rearrangement, where we have used the fact $\boldsymbol{\sigma}_p : (\mathbf{U} - \frac{1}{d}\mathrm{Tr}(\mathbf{U})\mathbf{I}) = 0$. From (2.17), one can check that the second integral is nonnegative and only vanishes when $\mathbf{U}$ is isotropic or $\boldsymbol{\sigma}_s = \mathbf{0}$. This means that the second integral with $\beta > 0$ dissipates the stored strain energy only when there are both shear stress and shear deformation.

4. Linearized model behavior. In this section, we will demonstrate the behavior of our nonlinear model with tissue rearrangement in its linearized regime. In the theory of small deformations, the adaptive displacement $\mathbf{u} = \mathbf{x} - \mathbf{y}$ is assumed to be small such that $\|\mathbf{u}\| \sim O(\epsilon)$ and $\|\nabla\mathbf{u}\| \sim O(\epsilon)$ are small where $\epsilon \ll 1$. Considering the characteristic time $T \sim 1/\beta$, we obtain the leading-order approximation of (3.1) by the evolution of $\mathbf{u}$

$$\frac{\partial \mathbf{u}}{\partial t} = \mathbf{v} - \beta\mathbf{u} \text{ with } \mathbf{u}(\mathbf{x},0) = \mathbf{0}, \tag{4.1}$$

where $\|\mathbf{v}\| \sim O(\epsilon)$ and the advection term is dropped as the higher order term of ϵ.

By assuming that the rate of tissue material growth is slower than the rate of tissue rearrangement, i.e., $\gamma/\beta \sim O(\epsilon)$, the active volumetric or areal variation can be written as $J_g = 1 + g$, where $g(\mathbf{x},t) \sim O(\epsilon)$ is the local active volume or areal increment. We can derive the evolution of g by the leading-order approximation of (3.4):

$$\frac{\partial g}{\partial t} = \gamma - \beta\nabla\cdot\mathbf{u} \text{ with } g(\mathbf{x},0) = 0, \tag{4.2}$$

where again, the advection term is dropped as the higher order term of ϵ.

The linearized stress from leading-order approximation of (2.17) can be written into the isotropic part and the deviatoric part

$$\boldsymbol{\sigma}_p = K(\nabla \cdot \mathbf{u} - g)\mathbf{I}, \tag{4.3}$$

$$\boldsymbol{\sigma}_s = \mu(\nabla \mathbf{u} + \nabla \mathbf{u}^{\mathrm{T}} - (2/d)(\nabla \cdot \mathbf{u})\mathbf{I}). \tag{4.4}$$

4.1. Viscoelastic stress relaxation. Differentiating (4.4) in time and using (4.1), we obtain the Maxwell model of viscoelastic materials

$$\boldsymbol{\sigma}_s + \frac{1}{\beta}\frac{\partial \boldsymbol{\sigma}_s}{\partial t} = \frac{\mu}{\beta}\Big(\nabla \mathbf{v} + \nabla \mathbf{v}^{\mathrm{T}} - \frac{2}{d}(\nabla \cdot \mathbf{v})\mathbf{I}\Big) \text{ with } \boldsymbol{\sigma}_s(\mathbf{x}, 0) = \mathbf{0}, \tag{4.5}$$

where $(\nabla \mathbf{v} + \nabla \mathbf{v}^{\mathrm{T}})$ defines the strain rate, β serves as the rate of stress relaxation, and the ratio μ/β plays the role of "effective" viscosity. Note here we use the time derivative $\partial \boldsymbol{\sigma}_s/\partial t$ in the linear approximation. In the general case of large deformation, the upper-convected time derivative $\overset{\triangledown}{\boldsymbol{\sigma}} = d\boldsymbol{\sigma}/dt - (\nabla \mathbf{v})^{\mathrm{T}} \cdot \boldsymbol{\sigma} - \boldsymbol{\sigma} \cdot (\nabla \mathbf{v})$ should be present. The Maxwell-like relaxation of deviatoric stress (4.5) reflects the fluidization of tissue by rearrangement, and hence we can use the rate of relaxation β to describe the fluidity of tissue. The tissue fluidization was also found by the linear viscoelastic model with the stress relaxation time scale coupled with the orientated cell division and death [41]. However, in general, the tissue rearrangement is not necessarily coupled with cell division but also can be facilitated by cell-cell topological transition and the reorganization of the cytoskeletal elements. In addition, not only is the relaxation independent of growth, but it also conserves the local mass. In our linearized model, the tissue viscosity can be independently modulated by the rate of rearrangement β. Henceforth we call β the *tissue fluidity*. See the summary and discussion section for a more detailed comparison with other works considering relaxation.

Differentiating (4.3) in time and using (4.1), we obtain the leading-order evolution of the isotropic stress (or the pressure)

$$\frac{\partial \boldsymbol{\sigma}_p}{\partial t} = K(\nabla \cdot \mathbf{v} - \gamma)\mathbf{I} \text{ with } \boldsymbol{\sigma}_p(\mathbf{x}, 0) = \mathbf{0}, \tag{4.6}$$

where K represents the bulk modulus. Clearly γ can influence $\partial \boldsymbol{\sigma}_p/\partial t$, which is consistent with the pressure dynamics description in [41]. Although the dynamics of $\boldsymbol{\sigma}_p$ does not include a dissipation term explicitly, the dissipation of $\boldsymbol{\sigma}_s$ through (4.5) can influence $\boldsymbol{\sigma}_p$ through the force balance equation $\nabla \cdot (\boldsymbol{\sigma}_s + \boldsymbol{\sigma}_p) = 0$, which means the rate of rearrangement β can influence both the pressure and deviatoric stress. This is different from [41], where an independent relaxation time of pressure is introduced to describe the tissue mechanics close to homeostasis.

4.2. Viscous tissue flow in the time scale of growth. If we assume the characteristic time $T \sim 1/\gamma \gg 1/\beta$, we have the quasi-steady-state relations from the leading order of (4.1), (4.2), and (4.5), i.e., $\mathbf{v} = \beta \mathbf{u}$, $\beta \nabla \cdot \mathbf{u} = \gamma$, and $\boldsymbol{\sigma}_s = \frac{\mu}{\beta}\Big(\nabla \mathbf{v} + \nabla \mathbf{v}^{\mathrm{T}} - \frac{2}{d}(\nabla \cdot \mathbf{v})\mathbf{I}\Big)$. Together with (4.3) and $\nabla \cdot (\boldsymbol{\sigma}_s + \boldsymbol{\sigma}_p) = 0$, we can derive the tissue behavior in mechanical equilibrium as viscous fluid

$$\frac{\mu}{\beta}\nabla^2 \mathbf{v} = K\nabla\left(g - \frac{\gamma}{\beta}\right) - \frac{\mu}{\beta}\left(1 - \frac{2}{d}\right)\nabla\gamma \quad \text{with the constraint} \quad \nabla \cdot \mathbf{v} = \gamma. \tag{4.7}$$

When $d = 2$, the last term on the right-hand side of (4.7) vanishes, and our model is similar to the viscoelastic fluid model [46], where the viscous tissue flow

is driven by the force generated by the gradient of myosin-dependent constriction. However, in our linearized fluid system, the rate of force-generating activities γ is the driver of the tissue dynamics, which results in a field of active volumetric or areal increment g and tissue flow $\mathbf{v}$. The tissue mechanics and flow can be modulated by the tissue fluidity β, together with the bulk modulus K and effective viscosity μ/β. The constraint $\nabla\cdot\mathbf{v}=\gamma$ implies incompressible tissue flow. However, the tissue can be under elastic compression or extension given that in general $J_e-1=\nabla\cdot\mathbf{u}-g+o(\epsilon)=\nabla\cdot\mathbf{v}/\beta-g+o(\epsilon)=\gamma/\beta-g+o(\epsilon)\neq 0$.

5. Growth of compressible tissues in radial symmetry. Now we apply our model to consider the growth of compressible tissues in radial symmetry with tissue rearranging activities. In the following we will present the results for the growth of a tissue spheroid ($d=3$). The results for the growth of a tissue disc ($d=2$) are qualitatively similar to those for a tissue spheroid and are included in the supplementary materials (Supplementary_Materials_r3.pdf [local/web 655KB]). We will first find an analytic equilibrium solution of the linearized system. Then we will perform numerical simulations to the nonlinear system and compare the results with the linear solutions.

5.1. Equilibrium solutions of the linearized system. We denote the solutions for the system of a tissue spheroid as functions of the radial coordinate r and time t, and write the system of equations (4.1)–(4.4) in spherical coordinates (r,θ,φ) with the force balance equation (2.19), the boundary conditions (2.20) at the tissue center $r=0$, and (2.21) at the free boundary $r=R(t)$, where $R(t)$ is the radius of tissue boundary at time t. Assuming that the active volumetric increment $g=J_g-1$, the adaptive displacement $u=r-y$, and $\partial u/\partial r$ are small, the linearized model of a growing tissue spheroid is given by

$$\begin{cases} \frac{\partial u}{\partial t}=v-\beta u,\\ \frac{\partial g}{\partial t}=\gamma-\beta\Big(\frac{\partial u}{\partial r}+2\frac{u}{r}\Big),\\ \frac{\partial\sigma_{rr}}{\partial r}+\frac{1}{r}(2\sigma_{rr}-\sigma_{\theta\theta}-\sigma_{\varphi\varphi})=0,\\ \sigma_{rr}=\frac{4}{3}\mu\Big(\frac{\partial u}{\partial r}-\frac{u}{r}\Big)+K\Big(\frac{\partial u}{\partial r}+2\frac{u}{r}-g\Big),\\ \sigma_{\theta\theta}=\sigma_{\varphi\varphi}=\frac{2}{3}\mu\Big(\frac{u}{r}-\frac{\partial u}{\partial r}\Big)+K\Big(\frac{\partial u}{\partial r}+2\frac{u}{r}-g\Big), \end{cases} \tag{5.1}$$

subject to stress-free initial conditions, fixed boundary condition at the origin $r=0$, and free moving boundary condition at $r=R(t)$

$$\begin{cases} u(r,0)=0,\quad g(r,0)=0,\\ v(0,t)=0,\\ \sigma_{rr}(R(t),t)=0,\quad \frac{dR}{dt}=v(R,t). \end{cases} \tag{5.2}$$

We consider the case where there is an equilibrium solution when $\partial u/\partial t=\partial g/\partial t=dR/dt=0$ in the system (5.1) and (5.2). We find the solution

$$v(r)=\frac{1}{r^2}\int_0^r\gamma(\xi)\xi^2d\xi,\quad g=\Big(1+\frac{4\mu}{3K}\Big)\frac{\gamma(r)}{\beta},\quad u(r)=\frac{v(r)}{\beta}. \tag{5.3}$$

The first equation provides the existence criterion for an equilibrium tissue radius R_{eq}, which is the existence of a positive solution of

$$G(R_{eq})=0,\quad \text{where}\quad G(r):=\int_0^r\gamma(\xi)\xi^2d\xi. \tag{5.4}$$

One can see R_{eq} is solely determined by γ through $G(r)$. Henceforth we call $G(r)$ the criterion function for the equilibrium size with respect to the growth rate γ. By assuming the continuity of γ, one can check there exists an equilibrium R_{eq} only when γ is partially positive and partially negative along the radial coordinate r.

We can also reconstruct the stresses and the elastic volume variation in equilibrium from the system (5.1):

$$\sigma_{rr} = -\frac{4\mu}{\beta}\frac{G(r)}{r^3}, \quad \sigma_{\theta\theta} = \frac{2\mu}{\beta}\Big(\frac{G(r)}{r^3} - \gamma(r)\Big), \quad J_e = 1 - \frac{4\mu}{3K}\frac{\gamma(r)}{\beta}. \tag{5.5}$$

Thus, the stresses are regulated by the differential growth $\gamma(r)$ and modulated by the effective viscosity μ/β in equilibrium. It is noted that the stresses in this linearized system are independent of the bulk modulus K. The isotropic stress (pressure) $\sigma_p = (\sigma_{rr} + 2\sigma_{\theta\theta})/3 = -(4\mu/3\beta)\gamma(r)$ is also dissipated with large β, suggesting the relaxation of the deviatoric stress also relaxes the pressure. This behavior is very different from the pressure relaxation dynamics in [41] where the pressure relaxation can follow an independent rate close to homeostasis. We can compute the tissue density in equilibrium by $\rho = \rho_0/J_e \cong \rho_0(1 + \frac{4\mu}{3K}\frac{\gamma(r)}{\beta})$. Thus, the spatial variation in density is modulated by K/μ, the bulk-to-shear-modulus ratio, and β/γ, the fluidity-to-growth-rate ratio. Both large K/μ and large β/γ result in small variation in density. The analytic equilibrium solutions of stress and density for the system of a tissue disc ($d = 2$) show similar qualitative behaviors (see the supplementary materials (Supplementary_Materials_r3.pdf [local/web 655KB])).

5.2. Nonlinear simulation with prescribed differential growth rate. To investigate the regulation of tissue size and mechanics in the nonlinear regime, we perform numerical simulations to the nonlinear model equations (2.17), (2.19), (3.1), and (3.4) with the fixed boundary condition (2.20) at $r = 0$ and the free boundary condition (2.21) at $r = R(t)$

$$\begin{cases} \frac{\partial y}{\partial t} + v\frac{\partial y}{\partial r} = \beta(r - y), \\ \frac{\partial J_g}{\partial t} + v\frac{\partial J_g}{\partial r} = J_g\Big[\gamma + \beta\Big(3 - (\frac{\partial y}{\partial r})^{-1} - 2(\frac{y}{r})^{-1}\Big)\Big], \\ \frac{\partial \sigma_{rr}}{\partial r} + \frac{1}{r}(2\sigma_{rr} - \sigma_{\theta\theta} - \sigma_{\varphi\varphi}) = 0, \\ \sigma_{rr} = \frac{2}{3}\mu J_g\Big((\frac{\partial y}{\partial r})^{-\frac{1}{3}}(\frac{y}{r})^{\frac{10}{3}} - (\frac{\partial y}{\partial r})^{\frac{5}{3}}(\frac{y}{r})^{\frac{4}{3}}\Big) + K\Big(J_g^{-1}(\frac{\partial y}{\partial r})^{-1}(\frac{y}{r})^{-2} - 1\Big), \\ \sigma_{\theta\theta} = \frac{1}{3}\mu J_g\Big((\frac{\partial y}{\partial r})^{\frac{5}{3}}(\frac{y}{r})^{\frac{4}{3}} - (\frac{\partial y}{\partial r})^{-\frac{1}{3}}(\frac{y}{r})^{\frac{10}{3}}\Big) + K\Big(J_g^{-1}(\frac{\partial y}{\partial r})^{-1}(\frac{y}{r})^{-2} - 1\Big), \\ \sigma_{\varphi\varphi} = \sigma_{\theta\theta}, \end{cases} \tag{5.6}$$

subject to the stress-free initial condition, the fixed boundary condition at $r = 0$, and free moving boundary condition at $r = R(t)$

$$\begin{cases} y(r,0) = r, \quad J_g(r,0) = 1, \\ v(0,t) = 0, \\ \sigma_{rr}(R,t) = 0, \quad \frac{dR}{dt} = v(R,t). \end{cases} \tag{5.7}$$

We nondimensionalize the system with respect to the characteristic length scale l, time scale T, and stress scale μ. Then the rescaled variables and parameters become $\tilde{r} = r/l$, $\tilde{y} = y/l$, $\tilde{R} = R/l$, $\tilde{t} = t/T$, $\tilde{v} = v/(l/T)$, $\tilde{\mu} = \mu/\mu = 1$, $\tilde{K} = K/\mu$, $\tilde{\sigma}_{rr} = \sigma_{rr}/\mu$, and $\tilde{\sigma}_{\theta\theta} = \sigma_{\theta\theta}/\mu$. We have considered the time scale $T \sim 1/\beta$ and $T \sim 1/\gamma$ in the discussion of linearized model behavior in section 4. However, since we will consider the growth rate γ coupled with nutrient transport in the simulations and study the effect of tissue fluidity β, we choose to not associate the time scale T with either

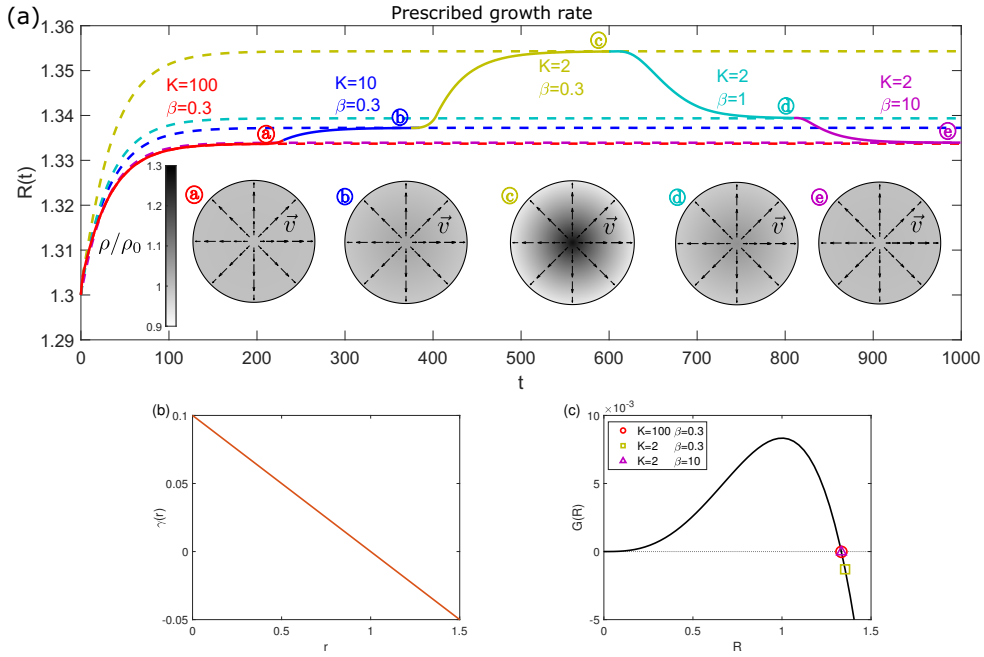

FIG. 2. (a) *Evolution of tissue radius $R(t)$ with dynamical modulation of β and K (solid line) and with different sets of constant K and β (dashed lines), with prescribed $\gamma(r) = 0.1(1-r)$. The grayscale color map in the disc panels* (a)–(e) *shows the scaled density ρ/ρ_0 profile within a tissue spheroid in equilibria for each set of parameters β and K. The arrows indicate the direction and relative magnitude of the tissue velocity.* (b) *The spatial profile of prescribed $\gamma(r)$. The location $r = 0$ corresponds to the tissue center.* (c) *Criterion function $G(R)$ with respect to $\gamma(r) = 0.1(1-r)$. The equilibrium size R_{eq} is marked (see legend) for different values of K and β. The equilibrium size R_{eq} deviates from the positive root of $G(R)$ for highly compressible and weakly fluidized ($K = 2$ and $\beta = 0.3$) tissues.*

rate. Instead, we have the nondimensionalized rates $\tilde{\beta} = \beta T$ and $\tilde{\gamma} = \gamma T$. Note that $\tilde{K}$ stands for the relative tissue compressibility. From now on, we will drop the tilde notation for the rescaled variables and parameters for simplicity of notation. We consider a prescribed differential growth rate $\gamma(r) = 0.1(1-r)$ in the Eulerian coordinates (Figure 2(b)), which indicates a differential growth with cell proliferation near the tissue center (for $r < 1$) and apoptosis away from the center (for $r > 1$). Note that here we choose the critical size at which $\gamma = 0$ to be the dimensional length ($r = 1$). This choice of γ gives the equilibrium tissue size of $R_{eq} = 4/3$ for the linear system from (5.4). We simulate the growth of tissue from a smaller size $R = 1.3$ until it reaches its mechanical equilibrium state.

To solve this nonlinear system, we first introduce the change of variable $r' = r/R(t) \in [0, 1]$ to the original system. The change of variable transforms the system from a moving domain $[0, R(t)]$ to a fixed domain $[0, 1]$. We discretize the new system by finite difference in space and time. The discretized system at each time point is solved by a semi-implicit iterative method. The details of the numerical method are not the core of this paper and are briefly presented in the supplementary materials (Supplementary_Materials_r3.pdf [local/web 655KB]).

5.2.1. Nonlinear effect on equilibrium tissue size. The evolution of tissue size $R(t)$ with different values of K and β is shown in Figure 2(a) (dashed lines). The results show that the equilibrium size of tissue for the nonlinear system, depending on

K and β, can deviate from the linear solution $R_{eq} = 4/3$. When K or β is large, the equilibrium size of nonlinear system is close to the linear solution; however, when K and β are both small, the tissue reaches a different equilibrium size. The disc panels in Figure 2(a) show the spatial profile of the rescaled tissue density ρ/ρ_0 (by grayscale color maps) and tissue flow v (by arrows) in equilibria. Due to the negative gradient of γ, the tissue density is larger near the center and smaller near the boundary, and tissue flows from the center to the boundary. It shows that the variation in density becomes significant when both K and β are small, in good agreement with the prediction from a linear model solution in equilibrium. Moreover, if we update K or β after the tissue reaches an equilibrium size, $R(t)$ will evolve to the new equilibrium corresponding to the updated values of K and β, as shown in Figure 2(a) (solid line). This also verifies that the equilibrium radius is independent of the initial size choice. Thus, we demonstrate that given $\gamma(r)$, the equilibrium tissue radius R_{eq} also depends on K and β. The nonlinear simulation results for a tissue disc ($d = 2$) display similar model behavior (see the supplementary materials (Supplementary_Materials_r3.pdf [local/web 655KB]) for more details).

We can understand why K and β modulate R_{eq} in the nonlinear model by the following analysis. When tissue is in mechanical equilibrium, its elastic volume variation $J_e = J/J_g$ or, equivalently, its density $\rho = \rho_0/J_e$ does not change locally (with respect to Eulerian coordinates), i.e., $\partial\rho/\partial t = \rho(\gamma - \nabla\cdot\mathbf{v}) - \mathbf{v}\cdot\nabla\rho = 0$. By rewriting this relation into $\gamma = \nabla\cdot\mathbf{v} + (1/\rho)\mathbf{v}\cdot\nabla\rho$ and integrating it in a tissue spheroid ($d = 3$) or disc ($d = 2$), we obtain

$$G(R_{eq}) = \int_0^{R_{eq}} \frac{1}{\rho}\Big(v\frac{\partial\rho}{\partial r}\Big) r^{d-1} dr \quad \text{with } G(R) = \int_0^R \gamma r^{d-1} dr, \tag{5.8}$$

where we have used the divergence theorem and $v(0,t) = 0$ and $v(R_{eq},t) = 0$.

For the strictly incompressible case, where $\rho \equiv \rho_0$, (5.8) is reduced to $G(R_{eq}) = 0$, where R_{eq} is solely determined by γ via the criterion function G, as in the linear case by (5.4). This is also the case when the tissue is nearly incompressible or highly fluidized (e.g., $K = 100$ or $\beta = 10$), where ρ is (almost) uniformly constant such that $\partial\rho/\partial r \cong 0$. However, when the tissue is highly compressible and weakly fluidized (e.g., $K = 2$ and $\beta = 0.3$), the right-hand side of (5.8) becomes negative since the nonlinear advection term $v\partial\rho/\partial r < 0$ everywhere except at $r = 0$ and $r = R_{eq}$. Thus the solution of R_{eq} to (5.8) is located at a different value where $G < 0$ (see Figure 2(c)). In [52], where the strictly incompressible tissue is considered, the tissue size can be modulated by external physical confinement through mechanical feedback mechanisms. Here, we show that the tissue material properties can modulate the tissue size without considering external compression or mechanical feedback mechanisms. To the best of our knowledge, this size-regulating behavior of tissues in a mechanically free growing environment due to its internal mechanical property and rearranging activity has not been predicted by previous models.

5.2.2. Regulation of tissue mechanics. Given the prescribed $\gamma(r) = 0.1(1 - r)$, the spatial distributions of the Cauchy stress components σ_{rr}, $\sigma_{\theta\theta}$, and the local elastic volume variation $J_e = (\rho/\rho_0)^{-1}$ are almost linear, under different combinations of β and K. Their distributions for $K = 2$ and $\beta = 10, 1, 0.3$ are shown in Figure 3 (solid lines). Since the nonlinear solutions of these variables are qausi-linear in r, they match closely with the linear model solutions (5.5) with different values of K and β (dashed lines in Figure 3). Overall, the tissue is under compression near the center (where the density is larger) and under extension near the boundary (where the density is smaller). When the tissue fluidity is large (large β), the Cauchy stress

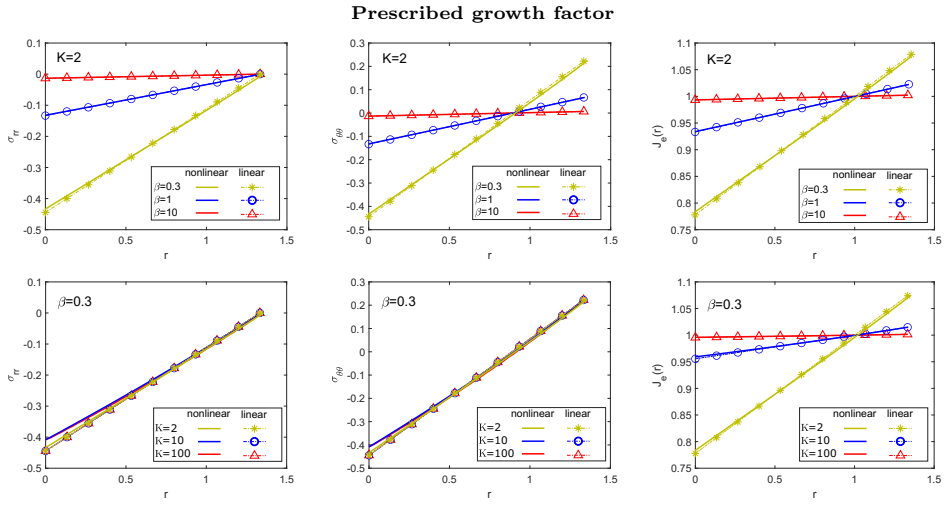

FIG. 3. *The Cauchy stress (σ_{rr} and $\sigma_{\theta\theta}$) and elastic volume variation $J_e = \rho_0/\rho$ in equilibria for different β (top row) and different K (bottom row) with prescribed $\gamma(r) = 0.1(1-r)$. Solid lines represent nonlinear simulation results; markers represent linear analytic solutions.*

components σ_{rr} and $\sigma_{\theta\theta}$ are dissipated and the elastic volume variation J_e is (almost) uniformly 1. When the tissue fluidity is small (small β), the gradients of σ_{rr}, $\sigma_{\theta\theta}$, and J_e are more significant. We also find that the stress in equilibrium is (almost) independent of K (see Figure 3), which is consistent with the analytical linear solution (5.5). Similar behavior in a tissue disc ($d = 2$) is shown in the supplementary materials (Supplementary_Materials_r3.pdf [local/web 655KB]).

6. Application to tissue growth coupled with chemical signals. Now we apply our nonlinear model to study the growth of radially symmetric tissue coupled with chemical signals. We will show the results for tumor spheroid growth ($d = 3$) in the following, and the results for epithelial disc growth ($d = 2$) are included in the supplementary materials (Supplementary_Materials_r3.pdf [local/web 655KB]). We consider that the growth rate γ is no longer prescribed as an a priori function but is coupled with a field of growth factor or nutrient that follows the reaction-diffusion process in the growing tissue domain. Supposing that $c(r,t)$ is the concentration of growth factor in the tumor spheroid, its dynamics follows

$$\begin{cases} \frac{1}{\lambda}\frac{\partial c}{\partial t} = L^2 \frac{1}{r^2}\frac{\partial}{\partial r}\left(r^2 \frac{\partial c}{\partial r}\right) - c \quad \text{for } 0 < r < R(t), \\ c(R(t),t) = 1, \quad \frac{\partial c}{\partial r}(0,t) = 0, \end{cases} \tag{6.1}$$

where we assume a Dirichlet boundary condition at the boundary and no flux boundary condition at the center such that the growth factor diffuses from the boundary to the central region. The turnover rate of the growth factor λ determines the characteristic time of the reaction-diffusion process and $L = \sqrt{D/\lambda}$ is the diffusion length, where D is diffusion coefficient. Assuming $\lambda \gg \gamma$, we can solve c by the quasi-steady-state approximation of (6.1) for tissue radius $R(t)$ at each time point. The obtained solution $c_R(r)$ is time-dependent via the moving domain boundary $R(t)$:

$$c_R(r) := c(r,t) = \frac{R(t)}{\sinh(R(t)/L)} \frac{\sinh(r/L)}{r}. \tag{6.2}$$

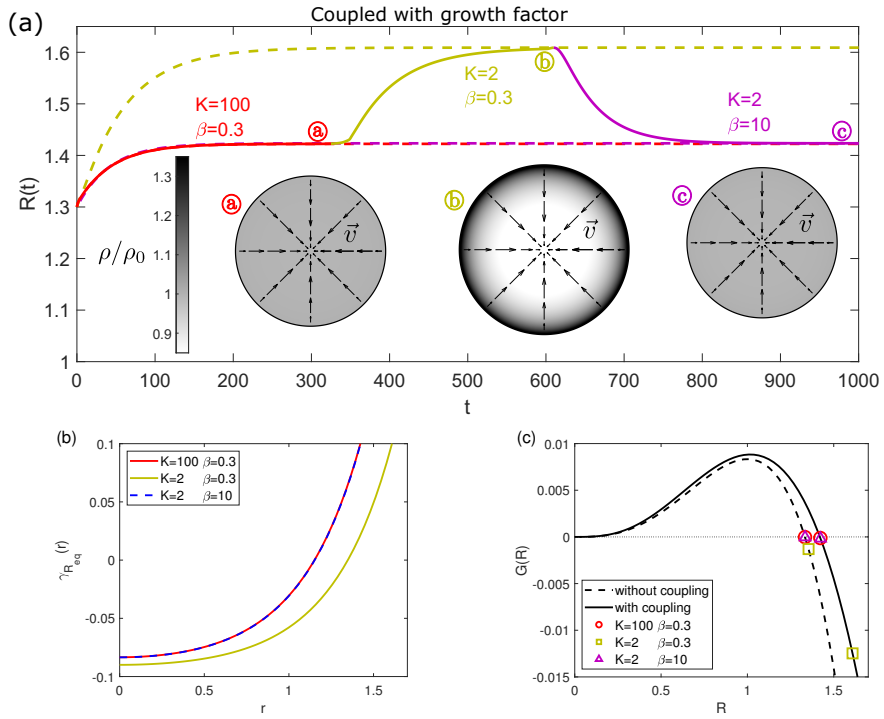

FIG. 4. (a) *Evolution of tumor size $R(t)$ with dynamical modulation of β and K (solid line) and with different sets of constant K and β (dashed lines), when γ is coupled with growth factor. Inset: the colored disk shows the scaled density ρ/ρ_0 profile within a tumor spheroid in equilibria* (a)–(c) *for each set of parameters β and K. The arrows indicate the direction and dimensionless magnitude of the velocity of tissue flow.* (b) *The spatial profile of $\gamma_{R_{eq}}(r)$ in equilibria when coupled with growth factor for different K and β.* (c) *Criterion function $G(R)$ for tumor equilibrium size when γ is prescribed a priori (dashed line) and coupled with growth factor (solid line). The equilibrium size R_{eq} is marked (see inset) for different values of K and β. The equilibrium size R_{eq} deviates from the root for highly compressible and weakly fluidized ($K=2$ and $\beta=0.3$) tumors. This deviation is pronounced when γ_R is coupled with growth factors.*

We consider that the local rate of active growth is coupled with the local concentration $c_R(r)$ in the simplified form of

$$\gamma_R(r) = c_R(r)\lambda_p - \lambda_a, \tag{6.3}$$

where $c_R\lambda_p$ and λ_a are the local rates of cell proliferation and apoptosis, respectively. Typical $\gamma_R(r)$ decreases from the boundary to the center of the tissue, and for a fixed location r_0, $\gamma_R(r_0)$ further decreases as $R(t)$ increases. Figure 4(b) shows $\gamma_{R_{eq}}(r)$ in equilibria with different R_{eq}. We perform simulations for the growth of a tumor spheroid with $\gamma = \gamma_R(r)$, with the parameter values $L = 0.3$, $\lambda_p = 0.2$, and $\lambda_a = 0.1$.

The evolution of a tumor spheroid with γ_R for different K and β is shown in Figure 4(a). The equilibrium tissue size can be modulated by K and β due to the same mechanism as explained in section 5.2.1. We show the equilibrium tumor size R_{eq} for different β and K in Figure 5. When the tumor is nearly incompressible ($K = 100$) or highly fluidized ($\beta = 10$), R_{eq} coincides with the root of the criterion function $G(R)$ (Figure 4(c)); when the tumor is highly compressible (small K) and weakly fluidized (small β), R_{eq} deviates from the root of $G(R)$ and increases to the

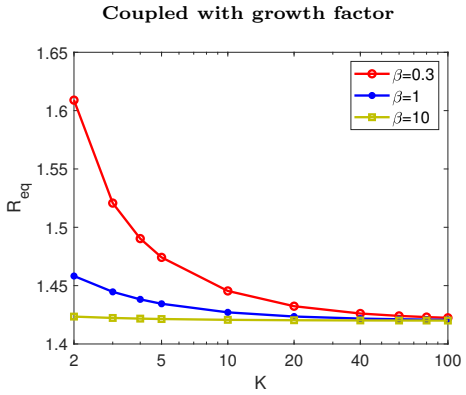

FIG. 5. *The equilibrium tumor size R_{eq} for different β and K.*

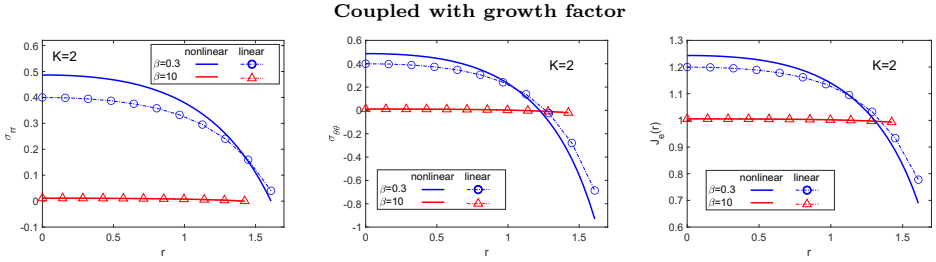

FIG. 6. *The Cauchy stress (σ_{rr} and $\sigma_{\theta\theta}$) and elastic volumetric change J_e in equilibria for different β when γ is coupled with growth factor. Solid lines represent nonlinear simulation results; markers represent linear analytic solutions.*

location where $G(R) < 0$. Compared to the case of prescribed γ (Figure 2(a)), the variation in R_{eq} for different K and β becomes significant in the case where $\gamma = \gamma_R$ is coupled with $c_R(r)$.

The positive gradient of γ_R results in a positive gradient in tissue density in equilibrium and induces inward tissue flow from the boundary to the center (see disc panels in Figure 4). Therefore, the tumor tissue is under tension near the center and compression near the boundary (Figure 6). The spatial distributions of the Cauchy stress components σ_{rr}, $\sigma_{\theta\theta}$, and the local elastic volume variation $J_e = (\rho/\rho_0)^{-1}$ with larger fluidity (e.g., $\beta = 10$) match well with the prediction from the linear solution equation (5.5). For smaller fluidity (e.g., $\beta = 0.3$), the nonlinear solutions obviously deviate from the linear solutions due to the stronger nonlinear effect. Moreover, we find that the stresses, unlike in the case of prescribed γ, can be also modulated by K, which is not the case for the linear solutions; see the supplemental materials (Supplementary_Materials_r3.pdf [local/web 655KB]) for more details illustrated with $d = 2$.

7. Summary and discussion. In this work, we presented a nonlinear biomechanical model for growing compressible tissues which couples the finite elasticity and growth with spatially dependent growth-promoting factors in an Eulerian frame. We have used the reference map techniques [10, 28], which track the inverse of the motion. This Eulerian approach based on the reference map is simpler from the computational perspective than the previous Maxwell-type model for stress relaxation. For example, previous Eulerian frameworks described the evolution of deformation gradient for

viscoelastic fluids [36, 35] and the elastic deformation gradient for deformable solids considering surface growth [39].

In [52], we have considered the tissue volume reductions as active processes of water efflux [24]. Here, we consider this tissue compressibility by its bulk modulus K, focusing on the solid structure that provides the elastic property approximated by the compressible neo-Hookean constitutive law. Without the constraint of strict incompressibility, we are able to demonstrate that the rearranging activity indeed dissipates the elastic energy in radial symmetry (where rotation can be neglected).

Tissue stress and strain relaxation can be regulated by cell divisions, or without division. In the first scenario, one can consider the (isotropic) growth as stress- or strain-dependent [53, 9, 19] to effectively relax the stresses, or consider the stress relaxation due to oriented division and apoptosis [5, 41] in continuum theories. In the second scenario, the stress can be relaxed by cell-cell and cytoskeleton rearrangements and thus can happen faster than the cell cycle. Our continuum model focuses on the second scenario and has introduced a rearrangement rate β (called tissue fluidity) which integrates several stress-relaxation events in time. Thus, this work differentiates itself from other works and has opened up a route to understanding how cytoskeleton and cell-cell junction activities regulate tissue growth and morphogenesis in large scales.

Ideally, one may be able to derive the macroscopic relaxation rate β from the activities of microscopic force-bearing molecules. For example, in the crosslinked cytoskeletal network, the evolution of binding/unbinding of the crosslinkers [17, 18] may give rise to a time varying equilibrium configuration defined by a permanent displacement of the network material points [14].

When the rearranging activities, such as cell topological transition and cytoskeletal reorganization, are much faster than the growth ($\gamma/\beta \ll 1$), we can approximate the nonlinear model by its linearized version. In the linear model, we have found Maxwell-type relaxation for the stress dynamics, where the relaxation time is scaled with $1/\beta$. This linear model is similar to the Maxwell-type viscoelastic model in [41], yet their relaxation time is growth-dependent (through anisotropic growth). If we consider the characteristic time $T \sim 1/\gamma \gg 1/\beta$, our model is reduced to an active viscous fluid model, which is similar to previous viscous fluid models [8, 46]. In our model, we have found that the effective tissue viscosity is given by μ/β, regulated by the shear modulus and the rearrangement rate. This relation connects the effective viscosity of tissues directly to the rearranging activities and elastic modulus when the characteristic time $T \sim 1/\gamma \gg 1/\beta$. In principle, the relaxation time $1/\beta$ is a result of chemomechanical regulation on the cell-cell contact and cytoskeletal evolution, and thus can change spatiotemporally. Take β as a function of stress, for example, which can be written as $\beta = \beta_0 + \beta_\sigma \times f_Y(\boldsymbol{\sigma})$, where β_0 models the stress-independent relaxation rate and $\beta_\sigma \times f_Y(\boldsymbol{\sigma})$ describes the stress-dependent relaxation rate with a yield criterion specified by f_Y. In the extreme case $\beta_0 = 0$, the tissue mechanics may behave like a plastic flow subject to a yield surface. However, in this case, it is not guaranteed that there will be an equilibrium reference map distribution that corresponds to a globally stress-free configuration, which is essentially different from the pure viscoelastic scenario. In general, by speculating the function β, we may derive a wide range of mechanical behaviors (e.g., viscoelastic, elastoplastic, and visco-elastoplastic). We leave this exploration to future work.

This reference-map based viscoelastic compressible tissue growth model is efficient to investigate in radially symmetric growth (e.g., tumor spheroids and epithelial discs growth), thanks to its relative simple formulation. We have applied this model to study the growth of compressible tissue spheroids and discs. When the ratio between

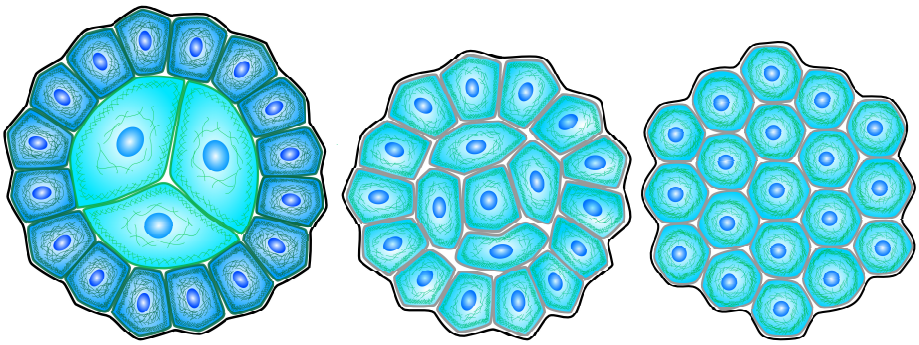

FIG. 7. *For weakly fluidized compressible tissue (left), the equilibrium size is larger than the incompressible (middle) or highly fluidized (right) tissue size, due to cell size change in response to the internal stress. See the text for more details.*

tissue fluidity and growth rate β/γ is large, we have presented the analytical steady-state solution of the linear model, and we have found that the tissue size is regulated solely by the spatial distribution of growth rate $\gamma(r)$ in radially symmetric tissues and the Cauchy stress distribution is regulated by the viscosity μ/β and $\gamma(r)$. In the nonlinear regime, we have found both the compressibility K/μ and the tissue fluidity β can influence the tissue equilibrium size in the mechanically free growing environment. When the tissue fluidity is small, as the tissue becomes more compressible, the tissue equilibrium size becomes larger. We have explained this effect as a nonlinear effect from the advection of the density gradient $v\frac{\partial \rho}{\partial r}$. Intuitively, we can also understand this result by the following. For weakly fluidized compressible tissue with larger proliferation at the boundary, we have higher density at the boundary and lower density at the center (e.g., see Figure 4). If we assume the cell density (cell number per volume) is proportional to the mass density (mass per volume), this means there are more proliferating cells at the tissue boundary which expand their sizes while flowing to the tissue center (see Figure 7). However, if the tissue is highly incompressible, cells will only change their shape but not their size in the tissue flow. With high fluidity, the stress level is low, thus cells do not change their size or shape during the flow. Thus, for highly incompressible or fluidized tissues, the equilibrium size will not be affected by the mechanics. This behavior is not observed in the incompressible model [52]. However, if an increased volume growth induced by tensile stress has been considered, the incompressible model may generate similar results. It is well documented that tumor cells on average become smaller when the tumor is under external compression [25, 12], thus tumor cells are compressible effectively. In experiments, one may validate our model prediction that the tissue fluidity can regulate the tumor size through modulating intercellular adherens junction level and cadherin trafficking [49] as has been done in fruit fly epithelia [26, 15].

This Eulerian frame model is ready to incorporate the coupling between the growth rate and stresses to investigate how tissue mechanical properties (e.g., compressibility and fluidity) influence tissue size regulation in radially symmetric growth (e.g., tumor spheroids and epithelial discs growth) via mechanical feedback mechanisms [44, 52]. Moreover, the presented model has the potential to describe the coupling between tissue growth and mechanics in higher dimensions beyond radial symmetry. In the future, we expect to extend the current Eulerian model to consider rearranging activities on higher dimensions beyond radial symmetry. For example,

it is interesting to study the effect of tissue fluidity on symmetry-breaking events to explain sophisticated shape formations [34, 45, 2].

REFERENCES

[1] T. Aegerter-Wilmsen, C. M. Aegerter, E. Hafen, and K. Basler, *Model for the regulation of size in the wing imaginal disc of Drosophila*, Mech. Dev., 124 (2007), pp. 318–326, https://doi.org/10.1016/j.mod.2006.12.005.

[2] M. B. Amar and F. Jia, *Anisotropic growth shapes intestinal tissues during embryogenesis*, Proc. Natl. Acad. Sci. USA, 110 (2013), pp. 10525–10530.

[3] D. Ambrosi, M. B. Amar, C. J. Cyron, A. DeSimone, A. Goriely, J. D. Humphrey, and E. Kuhl, *Growth and remodelling of living tissues: Perspectives, challenges and opportunities*, J. R. Soc. Interface, 16 (2019), https://doi.org/10.1098/rsif.2019.0233.

[4] D. Ambrosi and F. Mollica, *On the mechanics of a growing tumor*, Internat. J. Engrg. Sci., 40 (2002), pp. 1297–1316.

[5] R. Araujo and D. McElwain, *A linear-elastic model of anisotropic tumour growth*, European J. Appl. Math., 15 (2004), pp. 365–384.

[6] R. P. Araujo and D. S. McElwain, *A mixture theory for the genesis of residual stresses in growing tissues* II*: Solutions to the biphasic equations for a multicell spheroid*, SIAM J. Appl. Math., 66 (2005), pp. 447–467.

[7] P. V. Bayly, R. J. Okamoto, G. Xu, Y. Shi, and L. A. Taber, *A cortical folding model incorporating stress-dependent growth explains gyral wavelengths and stress patterns in the developing brain*, Phys. Biol., 10 (2013), 016005.

[8] F. Bosveld, I. Bonnet, B. Guirao, S. Tlili, Z. Wang, A. Petitalot, R. Marchand, P.-L. Bardet, P. Marcq, F. Graner, et al., *Mechanical control of morphogenesis by fat/dachsous/four-jointed planar cell polarity pathway*, Science, 336 (2012), pp. 724–727.

[9] S. Budday, P. Steinmann, A. Goriely, and E. Kuhl, *Size and curvature regulate pattern selection in the mammalian brain*, Extreme Mech. Lett., 4 (2015), pp. 193–198.

[10] G.-H. Cottet, E. Maitre, and T. Milcent, *Eulerian formulation and level set models for incompressible fluid-structure interaction*, ESAIM Math. Model. Numer. Anal., 42 (2008), pp. 471–492, http://www.esaim-m2an.org/10.1051/m2an:2008013.

[11] V. Cristini, J. Lowengrub, and Q. Nie, *Nonlinear simulation of tumor growth*, J. Math. Biol., 46 (2003), pp. 191–224, https://doi.org/10.1007/s00285-002-0174-6.

[12] M. Delarue, F. Montel, D. Vignjevic, J. Prost, J. F. Joanny, and G. Cappello, *Compressive stress inhibits proliferation in tumor spheroids through a volume limitation*, Biophys. J., 107 (2014), pp. 1821–1828, https://doi.org/10.1016/j.bpj.2014.08.031.

[13] E. G. B. R. O. S. Didier Bresch and T. Colin, *A Viscoelastic Model for Avascular Tumor Growth*, Conference Publications, 2009 (2009), pp. 101–108.

[14] K. Doubrovinski, M. Swan, O. Polyakov, and E. F. Wieschaus, *Measurement of cortical elasticity in drosophila melanogaster embryos using ferrofluids*, Proc. Natl. Acad. Sci. USA, 114 (2017), pp. 1051–1056.

[15] N. Founounou, R. Farhadifar, G. M. Collu, U. Weber, M. J. Shelley, and M. Mlodzik, *Tissue fluidity mediated by adherens junction dynamics promotes planar cell polarity-driven ommatidial rotation*, Nat. Commun., 12 (2021), pp. 1–16.

[16] Y.-C. Fung, *Biomechanics: Mechanical Properties of Living Tissues*, Springer Science & Business Media, New York, 2013.

[17] S. Fürthauer, B. Lemma, P. J. Foster, S. C. Ems-McClung, C.-H. Yu, C. E. Walczak, Z. Dogic, D. J. Needleman, and M. J. Shelley, *Self-straining of actively crosslinked microtubule networks*, Nat. Phys., 15 (2019), pp. 1295–1300.

[18] S. Fürthauer, D. J. Needleman, and M. J. Shelley, *A design framework for actively crosslinked filament networks*, New J. Phys., 23 (2021), 013012.

[19] K. E. Garcia, R. J. Okamoto, P. V. Bayly, and L. A. Taber, *Contraction and stress-dependent growth shape the forebrain of the early chicken embryo*, J. Mech. Behav. Biomed. Mater., 65 (2017), pp. 383–397.

[20] S. Göktepe, O. J. Abilez, K. K. Parker, and E. Kuhl, *A multiscale model for eccentric and concentric cardiac growth through sarcomerogenesis*, J. Theoret. Biol., 265 (2010), pp. 433–442, https://doi.org/10.1016/j.jtbi.2010.04.023.

[21] A. Goriely, *The Mathematics and Mechanics of Biological Growth*, Springer, New York, 2017.

[22] A. Goriely and M. Ben Amar, *Differential growth and instability in elastic shells*, Phys. Rev. Lett., 94 (2005), pp. 1–4, https://doi.org/10.1103/PhysRevLett.94.198103.

[23] C. Guillot and T. Lecuit, *Mechanics of epithelial tissue homeostasis and morphogenesis*, Science, 340 (2013), pp. 1185–1189, https://doi.org/10.1126/science.1235249.

[24] M. Guo, A. F. Pegoraro, A. Mao, E. H. Zhou, P. R. Arany, Y. Han, D. T. Burnette, M. H. Jensen, K. E. Kasza, J. R. Moore, et al., *Cell volume change through water efflux impacts cell stiffness and stem cell fate*, Proc. Natl. Acad. Sci. USA, 114 (2017), pp. E8618–E8627.

[25] G. Helmlinger, P. A. Netti, H. C. Lichtenbeld, R. J. Melder, and R. K. Jain, *Solid stress inhibits the growth of multicellular tumor spheroids*, Nat. Biotechnol., 15 (1997), p. 778.

[26] K. V. Iyer, R. Piscitello-Gómez, J. Paijmans, F. Jülicher, and S. Eaton, *Epithelial viscoelasticity is regulated by mechanosensitive e-cadherin turnover*, Curr. Biol., 29 (2019), pp. 578–591.

[27] G. W. Jones and S. J. Chapman, *Modeling growth in biological materials*, SIAM Rev., 54 (2012), pp. 52–118, https://doi.org/10.1137/080731785.

[28] K. Kamrin, C. H. Rycroft, and J. C. Nave, *Reference map technique for finite-strain elasticity and fluid-solid interaction*, J. Mech. Phys. Solids, 60 (2012), pp. 1952–1969, https://doi.org/10.1016/j.jmps.2012.06.003.

[29] E. Kröner, *Allgemeine kontinuumstheorie der versetzungen und eigenspannungen*, Arch. Ration. Mech. Anal., 4 (1959), pp. 273–334.

[30] T. Lecuit, P.-F. Lenne, and E. Munro, *Force generation, transmission, and integration during cell and tissue morphogenesis*, Annu. Rev. Cell Dev. Biol., 27 (2011), pp. 157–184.

[31] E. H. Lee, *Elastic-plastic deformation at finite strains*, Trans. ASME J. Appl. Mech., 54 (1969), pp. 1–6.

[32] L. LeGoff and T. Lecuit, *Mechanical forces and growth in animal tissues*, Cold Spring Harb. Perspect. Biol., 8 (2016), a019232.

[33] L. LeGoff, H. Rouault, and T. Lecuit, *A global pattern of mechanical stress polarizes cell divisions and cell shape in the growing drosophila wing disc*, Development, 140 (2013), pp. 4051–4059.

[34] B. Li, Y. P. Cao, X. Q. Feng, and H. Gao, *Surface wrinkling of mucosa induced by volumetric growth: Theory, simulation and experiment*, J. Mech. Phys. Solids, 59 (2011), pp. 758–774, https://doi.org/10.1016/j.jmps.2011.01.010.

[35] F.-H. Lin, C. Liu, and P. Zhang, *On hydrodynamics of viscoelastic fluids*, Comm. Pure Appl. Math., 58 (2005), pp. 1437–1471, https://doi.org/10.1002/cpa.20074.

[36] C. Liu and N. J. Walkington, *An Eulerian description of fluids containing visco-elastic particles*, Arch. Ration. Mech. Anal., 159 (2001), pp. 229–252, https://doi.org/10.1007/s002050100158.

[37] S. R. Lubkin and T. Jackson, *Multiphase mechanics of capsule formation in tumors*, J. Biomech. Eng., 124 (2002), pp. 237–243, https://doi.org/10.1115/1.1427925.

[38] F. Montel, M. Delarue, J. Elgeti, L. Malaquin, M. Basan, T. Risler, B. Cabane, D. Vignjevic, J. Prost, G. Cappello, et al., *Stress clamp experiments on multicellular tumor spheroids*, Phys. Rev. Lett., 107 (2011), 188102.

[39] S. K. Naghibzadeh, N. Walkington, and K. Dayal, *Surface growth in deformable solids using an Eulerian formulation*, J. Mech. Phys. Solids, 154 (2021), pp. 1–18, https://doi.org/10.1016/j.jmps.2021.104499.

[40] D. Nolan and J. McGarry, *On the compressibility of arterial tissue*, Ann. Biomed. Eng., 44 (2016), pp. 993–1007.

[41] J. Ranft, M. Basan, J. Elgeti, J.-F. Joanny, J. Prost, and F. Jülicher, *Fluidization of tissues by cell division and apoptosis*, Proc. Natl. Acad. Sci. USA, 107 (2010), pp. 20863–20868, https://doi.org/10.1073/pnas.1011086107.

[42] E. K. Rodriguez, A. Hoger, and A. D. McCulloch, *Stress-dependent finite growth in soft elastic tissues*, J. Biomech., 27 (1994), pp. 455–467, https://doi.org/10.1016/0021-9290(94)90021-3.

[43] S. Sadik and A. Yavari, *On the origins of the idea of the multiplicative decomposition of the deformation gradient*, Math. Mech. Solids, 22 (2017), pp. 771–772.

[44] B. I. Shraiman, *Mechanical feedback as a possible regulator of tissue growth*, Proc. Natl. Acad. Sci. USA, 102 (2005), pp. 3318–3323, https://doi.org/10.1073/pnas.0404782102.

[45] A. E. Shyer, T. Tallinen, N. L. Nerurkar, Z. Wei, E. S. Gil, D. L. Kaplan, C. J. Tabin, and L. Mahadevan, *Villification: How the gut gets its villi*, Science, 342 (2013), pp. 212–218.

[46] S. J. Streichan, M. F. Lefebvre, N. Noll, E. F. Wieschaus, and B. I. Shraiman, *Global morphogenetic flow is accurately predicted by the spatial distribution of myosin motors*, eLife, 7 (2018), e27454, https://doi.org/10.7554/eLife.27454.

[47] L. A. Taber, *Towards a unified theory for morphomechanics*, Philos. Trans. A, 367 (2009), pp. 3555–3583, https://doi.org/10.1098/rsta.2009.0100.

[48] T. Tallinen, J. Y. Chung, F. Rousseau, N. Girard, J. Lefèvre, and L. Mahadevan, *On the growth and form of cortical convolutions*, Nat. Phys., 12 (2016), pp. 588–593.
[49] J. J. West and T. J. Harris, *Cadherin trafficking for tissue morphogenesis: Control and consequences*, Traffic, 17 (2016), pp. 1233–1243.
[50] M. Wu and M. Ben Amar, *Growth and remodelling for profound circular wounds in skin*, Biomech. Model. Mechanobiol., 14 (2015), pp. 357–370, https://doi.org/10.1007/s10237-014-0609-1.
[51] S.-L. Xue, B. Li, X.-Q. Feng, and H. Gao, *Biochemomechanical poroelastic theory of avascular tumor growth*, J. Mech. Phys. Solids, 94 (2016), pp. 409–432.
[52] H. Yan, D. Ramirez-Guerrero, J. Lowengrub, and M. Wu, *Stress generation, relaxation and size control in confined tumor growth*, PLOS Comput. Biol., 18 (2022), e1010288.
[53] A. M. Zöllner, A. B. Tepole, and E. Kuhl, *On the biomechanics and mechanobiology of growing skin*, J. Theoret. Biol., 297 (2012), pp. 166–175.